Available online at www.sciencedirect.com

SCIENCE DIRECT®

Biochimica et Biophysica Acta 1665 (2004) 177–183

BIOCHIMICA ET BIOPHYSICA ACTA
BBA

http://www.elsevier.com/locate/bba

Spin-labelled vacuolar-ATPase inhibitors in lipid membranes

Neil Dixon[b], Tibor Páli[a], Terence P. Kee[b], Derek Marsh[a,*]

[a]*Max-Planck-Institut für biophysikalische Chemie, Abt. Spektroskopie, 37070 Göttingen, Germany*
[b]*Department of Chemistry, University of Leeds, Leeds LS2 9JT, UK*

Received 26 February 2004; received in revised form 5 August 2004; accepted 9 August 2004
Available online 21 August 2004

Abstract

Two spin-labelled derivatives of the 5-(2-indolyl)-2,4-pentadienoyl class of inhibitors of the vacuolar ATPase have been synthesised and their EPR properties characterised in phospholipid membranes. One spin-labelled inhibitor is the amide derivative of pentadienic acid and 4-amino-TEMPO (INDOL6), and the other is the 3-hydroxymethyl-PROXYL ester (INDOL5). The response of the EPR spectra to the chain-melting transition of dimyristoyl phosphatidylcholine (DMPC) bilayers demonstrates that both derivatives incorporate in phospholipid membranes. The axially anisotropic EPR spectra of INDOL6 in fluid DMPC membranes indicate that the indolyl-pentadienoyl inhibitors intercalate between the lipid chains, in the membrane. INDOL5, designed to possess additional internal segmental mobility, exhibits more nearly isotropic motion of the spin-label moiety in fluid membranes than does INDOL6. The EPR characteristics of INDOL5 are therefore well suited to detecting specific ligand–protein interactions. Progressive saturation EPR experiments with polar and hydrophobic relaxation agents (aqueous Ni^{2+} and oxygen) show that the nitroxide group is buried in the membrane, with the indole moiety providing the anchor at the membrane polar–apolar interface. Rates of spin-label reduction by externally added ascorbate confirm this assignment. These two spin-labelled derivatives provide complementary EPR probes of the lipid environment (INDOL6), and of ligand–protein interactions (INDOL5), for this class of V-ATPase inhibitor.

Keywords: Spin label; Electron spin resonance (ESR); Lipid bilayer; V-ATPase; Indole inhibitor

1. Introduction

Inhibition of the osteoclast variant of the vacuolar ATPase (V-ATPase) potentially provides a therapeutic strategy to combat bone resorption in osteoporosis. Of the 5-(2-indolyl)-2,4-pentadienoyl family of inhibitors, the 1,2,2,6,6-pentamethyl-piperidin-4-yl derivative shown in Fig. 1 (INDOL0) has an IC_{50} of 29 nM for inhibition of the V-ATPase in chicken osteoclasts, and exhibits a selectivity for the osteoclast enzyme over other V-ATPases [1]. To serve as a spin-label EPR reporter of the membrane environment and site of action for this class of inhibitor, we have synthesised INDOL6, the nitroxyl variant of INDOL0 [2]. Subsequent EPR analysis shows INDOL6 to be highly ordered in fluid lipid membranes, and led to the synthesis of a complementary derivative, INDOL5. The latter spin label was designed to possess additional internal molecular rotational freedom, compared with INDOL6, and hence to be better suited to the detection of inhibitor ligand–protein interactions.

In the present paper, we describe the EPR properties of the two spin-labelled inhibitors in phospholipid bilayer membranes of dimyristoyl phosphatidylcholine (DMPC). Spectral line shapes are used to deduce the mode of insertion of the inhibitor in the membrane. Relaxation enhancement agents are used to localise the spin label group within the bilayer. Chemical reduction by aqueous ascorbate is further used to determine penetration depth and directionality of insertion. This study characterises the ordering, orientation, location and mobility of the indolylpentadienoyl inhibitors in the lipid milieu of biological membranes. It therefore provides the requisite background for use of these

* Corresponding author. Tel.: +49 551 201 1285; fax: +49 551 201 1501.
E-mail address: dmarsh@gwdg.de (D. Marsh).

0005-2736/$ - see front matter © 2004 Elsevier B.V. All rights reserved.
doi:10.1016/j.bbamem.2004.08.001

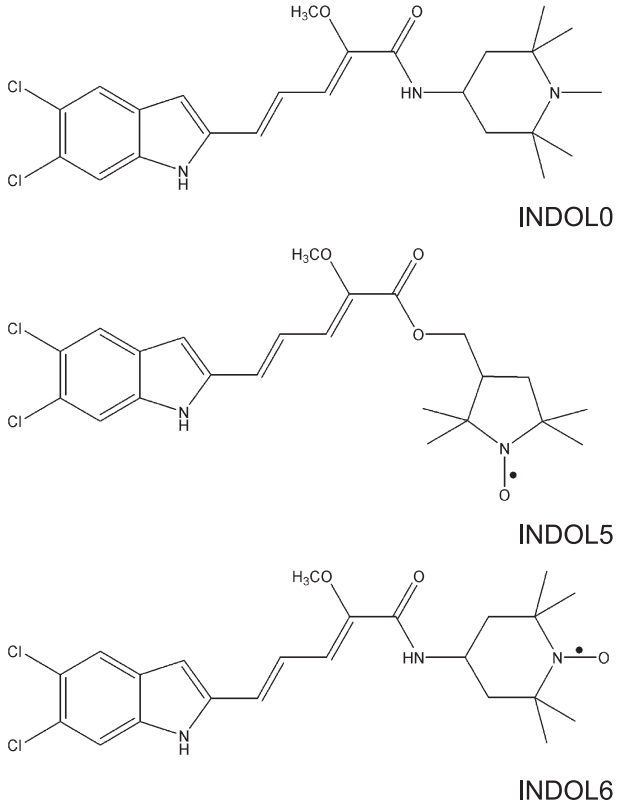

Fig. 1. Chemical structures of 5-(2-indolyl)-2,4-pentadienoyl derivatives.

molecules to probe the inhibitor binding sites in reconstituted V-ATPases and vacuolar membranes.

2. Materials and methods

2.1. Materials

DMPC was obtained from Avanti Polar Lipids (Alabaster, AL). Spin-labelled phosphatidylcholines *n*-PCSL (1-acyl-2-[*n*-(4,4-dimethyloxazolidine-*N*-oxyl)]stearoyl-*sn*-glycero-3-phosphocholine) were synthesised as described in Ref. [3]. Spin-labelled cholestane (3-spiro-[2′-(4′,4′-dimethyloxazolidine-*N*-oxyl)]-cholestane, CSL) was obtained from Syva (Palo Alto, CA). HEPES buffer and sodium ascorbate were from Sigma Chemical Co. (St. Louis, MO).

2.2. Synthesis of spin-labelled 5-(2-indolyl)-2, 4-pentadienoyls

2.2.1. INDOL6

(2*Z*,4*E*)-5-(5,6-Dichloro-2-indolyl)-2-methoxy-2,4-pentadienoic acid [4] (100 mg, 0.32 mmol), 1-hydroxybenzotriazole (48 mg, 1.1 eq), and *N*-[3-(dimethylamino)-*N*-ethylcarbodiimide hydrochloride (68 mg, 1.1 eq) dissolved in CH_3CN (3 ml) and tetrahydrofuran (THF; 1 ml) were heated at 40 °C under N_2 for 1 h. After which, the mixture was warmed to 60 °C, 4-amino-2,2,6,6-tetramethylpiperidinoxy free radical (66 mg, 1.2 eq) was added, and then refluxed for 1 h. After cooling, the solvent was removed under reduced pressure, the residue treated with 10% NaOH, extracted (EtOAc), dried ($MgSO_4$), and concentrated to give the crude product. The latter was purified by flash column chromatography, eluted with EtOAc/Petrol (7:3), to give (2*Z*,4*E*)-5-(5,6-dichloro-2-indolyl)-2-methoxy-*N*-[4-(2,2,6,6-tetramethylpiperidinoxy]-2,4-pentadienamide (118 mg, 79%). (Full characterisation is reported in Ref. [2].) The IC_{50} of INDOL6 for inhibition of yeast V-ATPase is ca. 10–30 μM, as compared with ca. 3 μM for the parent compound INDOL0.

2.2.2. INDOL5

$SOCl_2$ (58 μl, 2.5 eq) was added to a suspension of 5-(5,6-dichloro-2-indolyl)-2-methoxy-2,4-pentadienoic acid (99 mg, 0.317 mmol) in THF (15 ml) and heated under reflux for 2 h, allowed to cool, and solvents removed under reduced pressure to give a green crystalline solid. This was dissolved in THF (3 ml) and treated with 1-oxyl-2,2,5,5-tetramethyl-3-hydroxy-methylpyrrolidine (15 mg, 0.35 eq), dimethylaminopyridine (38 mg, 0.3 eq), stirred at room temperature for 7 h, and then heated under reflux for 3 h. The reaction was allowed to cool to room temperature, diluted with CH_2Cl_2, washed with sat. $NaHCO_3$ solution (3 ml) and extracted with CH_2Cl_2 (3×15 ml). The combined organics were dried ($MgSO_4$) and concentrated under reduced pressure to give the crude product, which was purified by flash column chromatography (EtOAc/Petrol, 1:1) to give a dark green crystalline solid (19 mg, 47%). Analysis by electro-spray mass spectrometry showed the major peak at M^++35, presumably arising from HCl addition to the desired ester product. (For full characterisation, see Ref. [5]).

2.3. Sample preparation

Lipid (ca. 1 mg) and spin label (at a relative concentration of <1 mol%) were codissolved in dichloromethane or chloroform–methanol. The solution was dried down in a nitrogen gas stream, and traces of the residual solvent were removed by evacuating overnight. The dry lipid was suspended in 50 μl of 40 mM HEPES, pH 7.0 buffer by vortexing at a temperature above the chain-melting transition of 24 °C. The lipid dispersion was then filled into a 50-μl, 1-mm i.d., glass capillary, and concentrated by pelletting in a benchtop centrifuge at 3000 rpm for 15 min. Excess supernatant was removed, the sample trimmed to 5-mm length, and the capillary was flame-sealed. For samples used in progressive saturation experiments, buffers and lipid dispersions were saturated with either argon or oxygen, and the sample capillaries were flushed with either argon or oxygen, as required.

For experiments to determine the rate of spin-label reduction by ascorbate, lipid dispersions were not centrifuged. The reaction was initiated by adding ascorbate from a concentrated stock solution to the lipid dispersion in the sample capillary, mixing, and then transferring the capillary immediately to the spectrometer.

2.4. EPR spectroscopy

EPR spectra were recorded on a Bruker EMX 9-GHz spectrometer, equipped with nitrogen gas-flow temperature regulation. Sample capillaries were accommodated in standard quartz EPR tubes which contained light silicone oil for thermal stability. Samples, 5 mm in length, were centred in the rectangular cavity resonator. Temperature was monitored by a fine-wire thermocouple situated in the silicone oil at the top of the EPR resonator. Progressive saturation experiments were performed by recording the conventional first-harmonic in-phase spectrum (V_1-display) as a function of the incident microwave H_1-field at the sample. Calibration of the H_1-field and correction for inhomogeneities were performed as described in Ref. [6].

3. Results and discussion

3.1. Spectra of INDOL6 and INDOL5 in DMPC membranes

The characteristic sensitivity of spin-label EPR spectra to membrane dynamics [7] allows information on the membrane environment of the nitroxide-labelled V-ATPase inhibitors to be obtained from the EPR line shapes. Fig. 2 gives the EPR spectra of INDOL6, the shorter amide-linked, piperidine nitroxide derivative of the indolyl inhibitor, in bilayer membranes of DMPC. At low temperature, e.g., 6 °C, the spectra correspond to a strongly immobilised spin label, although not completely at the rigid limit. This is characteristic of the ordered gel-state of lipid bilayer membranes. At around 25 °C, the total spectral extent decreases considerably, as a result of (partial) motional averaging in response to the chain-melting transition of the DMPC bilayers. In the fluid state, above the phase transition, the EPR spectra of INDOL6 still possess considerable residual anisotropy. They do not approximate to a sharp, three-line isotropic hyperfine spectrum. This spectral anisotropy indicates that the INDOL6 molecule is oriented by the fluid lipid chains, with relatively little internal segmental motion. Both the ordering of INDOL6 in the fluid, liquid-crystalline phase of the lipid membrane and the cooperative response to the phase transition (see Fig. 3) indicate that the spin-labelled indolyl derivative is intercalated between the lipid chains of the membrane.

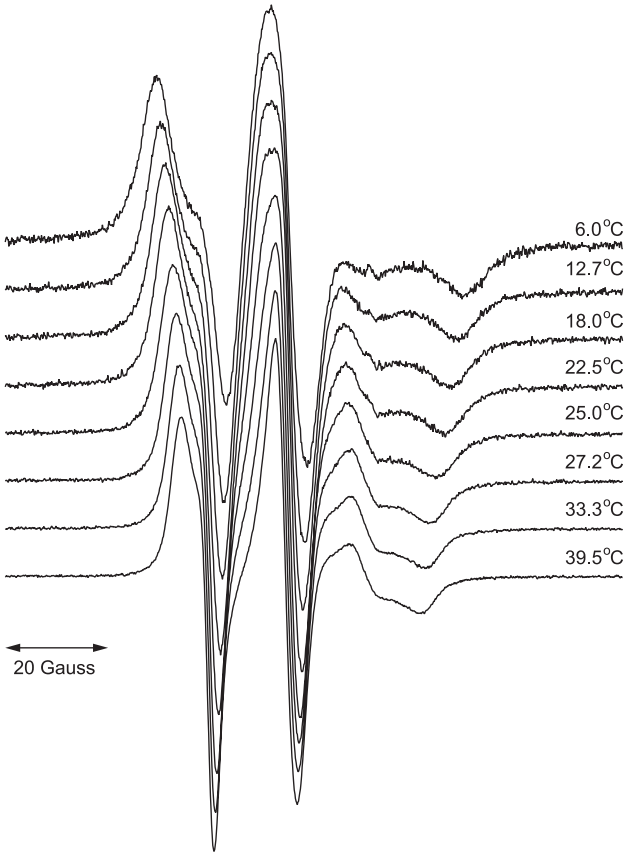

Fig. 2. EPR spectra of amide spin-labelled 5-(2-indolyl)-2,4-pentadienoyl derivative INDOL6 in membranes of DMPC at the temperatures indicated. Total scan width=120 G.

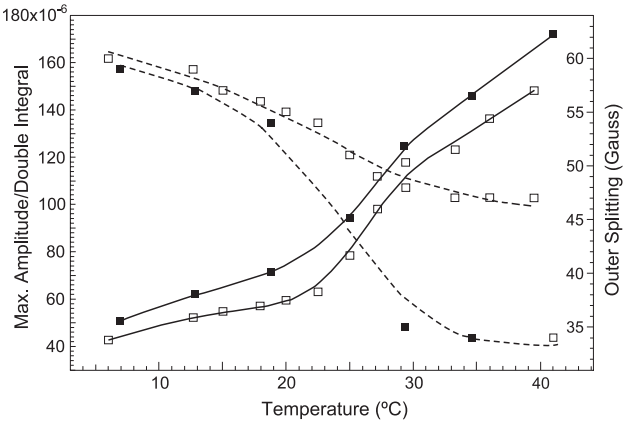

Fig. 3. Temperature dependence of the normalised maximum EPR-amplitude (solid lines) and outer hyperfine splitting, $2A_{max}$ (dashed lines), for the INDOL6 (open symbols) and INDOL5 (solid symbols) spin-labelled derivatives in DMPC membranes. The EPR-amplitude is normalised to the total spin intensity by using the double integral of the conventional first-derivative spectrum.

Fig. 4 gives the EPR spectra of INDOL5, the longer, ester-linked pyrrolidine nitroxide derivative, in DMPC bilayer membranes. The spectra of INDOL5 in the gel phase at low temperature (e.g., 6 °C) are again indicative of strong immobilisation, but not quite to the same extent as for INDOL6. At the chain-melting transition, around 25 °C (see Fig. 3), the spectra of INDOL5 narrow considerably—much more so than do those of INDOL6. Above the phase transition, in the fluid membrane phase, the spectra of INDOL5 rapidly come to approximate an isotropic, three-line spectrum with relatively narrow hyperfine lines, although these remain differentially broadened. This contrasts with the behaviour of INDOL6 in the fluid phase, where its amplitude of rotation is still limited anisotropically.

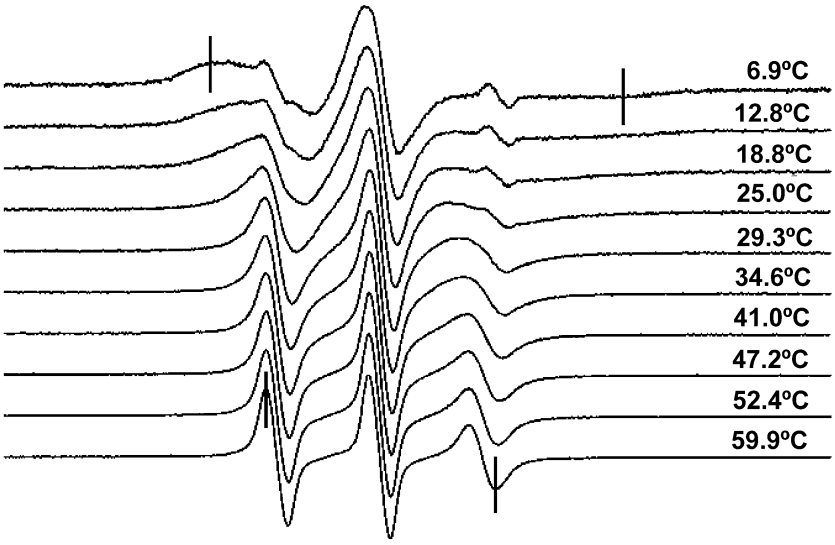

Fig. 4. EPR spectra of ester spin-labelled 5-(2-indolyl)-2,4-pentadienoyl derivative INDOL5 in membranes of DMPC at the temperatures indicated. Total scan width=120 G.

The difference in rotational freedom of the spin label group between the INDOL6 and INDOL5 derivatives in fluid membranes must be attributed to the additional single bond in the link between the nitroxide ring and indolyl conjugated system. Thus, the enhanced rotational freedom of INDOL5 arises from increased segmental motion within the molecule. These contrasting spectral properties of the two indolyl-pentadienoyl derivatives furnish complementary probes of the membrane environment of the V-ATPase inhibitor. By virtue of its pronounced spectral anisotropy, INDOL6 is expected to be extremely sensitive to the nature of the lipid membrane environment in which the inhibitor is situated. On the other hand, INDOL5 has a rather narrow isotropic spectrum in fluid lipid membranes. This offers the opportunity of detecting specific ligand–protein interactions with INDOL5, by resolving a second immobilised spectral component. The latter situation is similar to the direct detection of lipid–protein interactions by using lipids spin-labelled close to the chain terminal methyl group [8].

3.2. Environmental polarity

The isotropic hyperfine splitting of the nitroxide, a_o^N, is unaffected by molecular motion, but is sensitive to environmental polarity and to hydrogen bonding (e.g., to water)—see, e.g., Ref. [7]. The values of a_o^N for INDOL6 and INDOL5 in solvents of different polarity and H-bonding capacity are given in Table 1. These values are determined simply from the baseline-crossing points of the first-derivative EPR spectra in these isotropic, non-viscous solvents. For both spin labels, the isotropic hyperfine splittings decrease from the highly polar, hydrogen-bonding solvent water (dielectric constant=80) to the apolar, aprotic solvent chloroform (dielectric constant=5). Those in a $CHCl_3$/MeOH (2:1 v/v) solvent mixture are intermediate. The values of a_o^N for INDOL6 are consistently higher than those for INDOL5, in each solvent. This corresponds to an intrinsic difference in spin-density distribution between nitroxides with the six-membered piperidine ring and the five-membered pyrrolidine ring.

The value of a_o^N for INDOL5 in DMPC bilayer membranes can be obtained from the baseline crossings in the symmetrical, isotropic, three-line, EPR spectra recorded at high temperature (see Fig. 4). The spectra of INDOL6 in DMPC bilayer membranes remain anisotropic, but of axial symmetry, even up to high temperatures (see Fig. 2). In this latter case, the value of a_o^N was obtained from the isotropic average: $a_o^N=1/3(A_{//}+2A_{\perp})$. Here $A_{//}$ and $A_{\perp}$ are the outer and inner hyperfine splittings that correspond to magnetic field orientations parallel and perpendicular, respectively, to the symmetry axis (i.e., to the membrane normal). Measurements were made at sufficiently high temperatures to ensure that the values of a_o^N were independent of temperature, i.e., free of artifacts from slow motion. It is seen from Table 1 that the values of a_o^N for INDOL6 and INDOL5 lie between the values in water and in the hydrophobic solvent chloroform. Both correspond to an effective environmental polarity that is similar to that in $CHCl_3$/MeOH (2:1 v/v). This indicates that the nitroxide group of INDOL6 and INDOL5 is not exposed directly to water but is buried within the membrane, at least partially.

Table 1
Isotropic ^{14}N-hyperfine splitting constants (a_o, Gauss) of the INDOL6 and INDOL5 spin-labelled inhibitors in different environments

Host	INDOL6	INDOL5
Water	16.7	16.2
$CHCl_3$/MeOH (2:1 v/v)	16.3	15.2
$CHCl_3$	15.9	14.8
DMPC bilayer	16.3	15.1

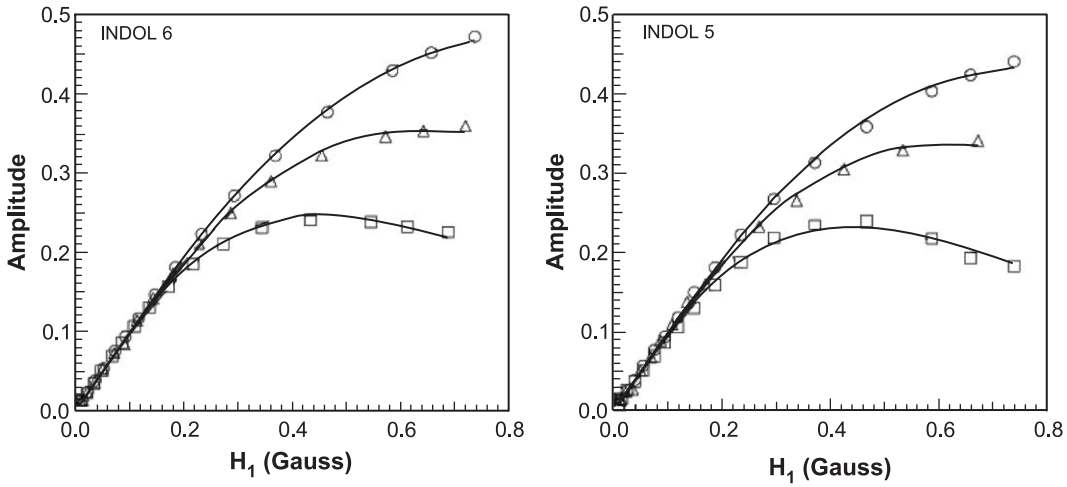

Fig. 5. Saturation curves, as a function of the H_1-microwave field strength, for the amplitude of the central (m_I=0) line in the EPR spectrum of INDOL6 (left) and INDOL5 (right) spin-labelled derivatives in DMPC membranes that are suspended in 40 mM HEPES buffer, pH 7.0, at 15 °C. Data are given for samples saturated with argon (□) or oxygen (○), and for argon-saturated samples in the presence of 30 mM $NiSO_4$ (△). Solid lines are nonlinear, least-squares fits of Eq. (1), with ε=1.5.

3.3. Accessibility to polar and hydrophobic relaxation agents

As discussed in the previous sections, the EPR line shapes demonstrate that the indolyl-pentadienoyl inhibitors intercalate and are ordered between the lipid chains. To determine the vertical location of the inhibitors in the membrane and, indeed, the directionality of insertion into the membrane, it is necessary to locate the position of the spin-label nitroxyl moiety in the membrane. In this section, we describe experiments with a relaxation agent that is confined essentially to the aqueous phase ($NiSO_4$), and a hydrophobic relaxant (molecular oxygen) that concentrates in the interior of the membrane (see, e.g., Ref. [9]).

Fig. 5 shows saturation curves for the amplitude of the central line in the EPR spectra of INDOL6 and INDOL5 in DMPC, as a function of increasing intensity of the H_1-microwave field. Saturation curves are given for samples in the absence (i.e., argon-saturated) and in the presence of the paramagnetic relaxation agents: either saturated with molecular oxygen or in 30 mM $NiSO_4$ saturated with argon. The alleviation of saturation of the spin-label amplitude at high H_1-field in the presence of the relaxation agents is clearly evident in Fig. 5. Oxygen is more effective than $NiSO_4$ in inducing relaxation enhancement. This suggests immediately that the nitroxide groups of INDOL6 and INDOL5 are located in the hydrophobic interior of the membrane.

The solid lines in Fig. 5 represent nonlinear least-squares fits of the following dependence of the spectral amplitude, A, on H_1-field:

$$A = (A_0 H_1)/\left(1 + \gamma_e^2 H_1^2 T_1 T_2\right)^{\varepsilon} \quad (1)$$

where γ_e is the electron gyromagnetic ratio, T_1 is the spin-lattice relaxation time, and T_2 is the transverse (or spin–spin) relaxation time. It is assumed that ε=1.5 for the central EPR amplitude in the fitting (which corresponds to purely Lorentzian line shapes), because the data are not sufficiently precise to use ε as a fitting parameter (see, e.g., Ref. [10]). From the fits it is possible to obtain values for the composite T_1T_2 relaxation time product (see, e.g., Ref. [11]).

Fig. 6 shows the relaxation rate enhancements obtained for the 5-PCSL and 14-PCSL spin labels in DMPC membranes, where the spin label group is on the n=5 or n=14 C-atom in the sn-2 chain of phosphatidylcholine. Horizontal bars in Fig. 6 indicate the corresponding corrected relaxation enhancements for the INDOL6 and INDOL5 inhibitors. Although there is some scatter in the data from the two labels, and between fluid and gel-phase membranes, the results of Fig. 6 indicate very clearly that

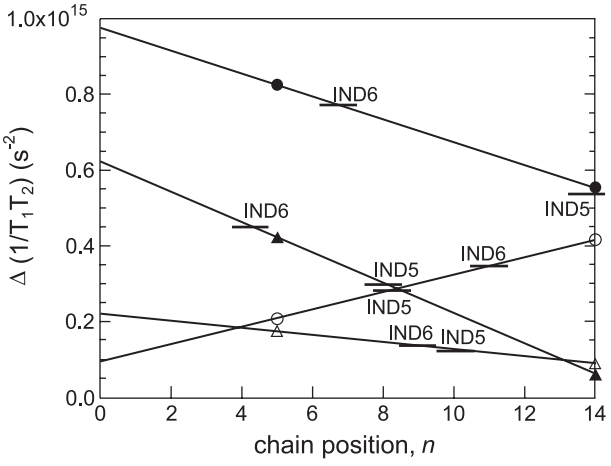

Fig. 6. Relaxation rate enhancement, $\Delta(1/T_1T_2)$, as a function of spin-label position, n, for n-PCSL in DMPC membranes at 15 °C (open symbols) and 40 °C (solid symbols) in the presence of oxygen (circles) or $NiSO_4$ (triangles) relaxation agents. Horizontal bars are the corresponding $\Delta(1/T_1T_2)$ rate enhancements for the indolyl spin-labelled derivatives, INDOL6 and INDOL5, as indicated, under the same conditions.

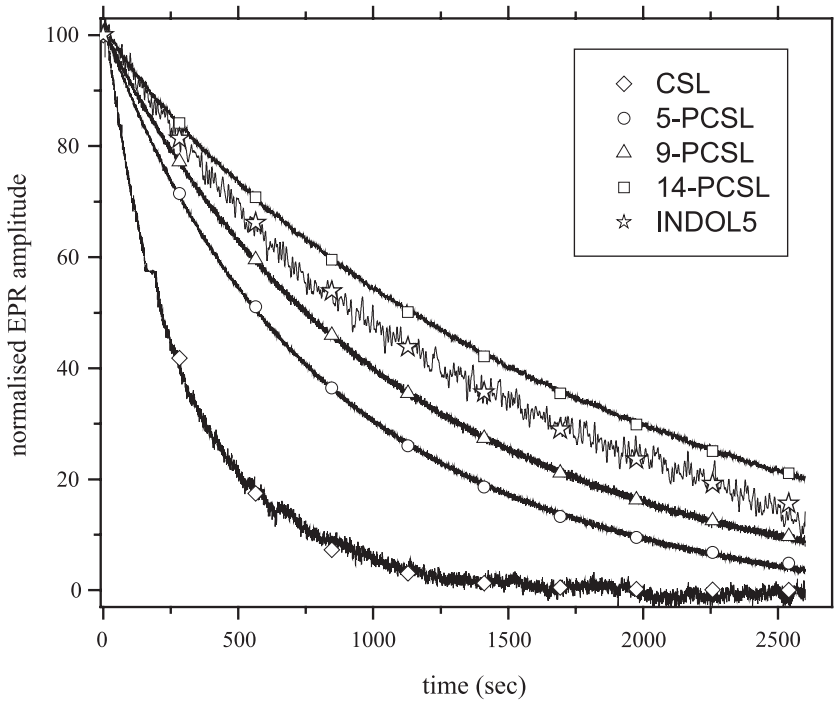

Fig. 7. Decay curves for spin-label lipids, *n*-PCSL and CSL, and indolyl derivative, INDOL5, in DMPC membranes in the presence of 10 mM ascorbate at 30 °C. The height of the central EPR line is plotted against time after addition of ascorbate. Symbols are single-exponential fits.

nitroxide groups of both indolyl inhibitors, INDOL6 and INDOL5, are located in the hydrocarbon interior of the membrane. This implies that both nitroxyl derivatives are anchored in the membrane with their indole groups at the polar–apolar interface of the membrane, and the nitroxide ring directed inwards. This is in agreement with the interfacial location of numerous tryptophan side-chain indoles in transmembrane proteins [12,13] and small peptides [14], as well as several indole-containing amphiphiles [15].

3.4. Reduction of membrane-bound INDOL5 and INDOL6 by ascorbate

The rates of chemical reaction of membrane-embedded spin labels by ascorbate permeating from the aqueous phase afford a means for determining the insertion depth of the spin label in the membrane [16]. Fig. 7 gives decay curves of the EPR amplitude for the INDOL5 derivative, and various spin-labelled lipids, on addition of 10 mM ascorbate to the membrane suspensions. The decays are exponential with a pseudo first-order rate constant of $k_1^{\mathrm{eff}}=k_2[\mathrm{asc}]_o$, where k_2 is the second-order rate constant and $[\mathrm{asc}]_o$ is the constant concentration of ascorbate in the aqueous phase. For the spin-labelled lipids, the dependence of the decay rate on depth in the membrane is clearly evident. The fastest decay is for spin-labelled cholestane (CSL), where the nitroxide group is located at the membrane–water interface (i.e., $n\equiv 0$).

Fig. 8 gives the half-times for reduction of the different spin-labelled lipids in DMPC membranes in the presence of 10 mM ascorbate. To compare with the corresponding values for the INDOL6 and INDOL5 spin labels, it is necessary to correct for the differences in reactivity with ascorbate of the different nitroxide moieties. The six-membered piperidine ring nitroxides are reduced much more rapidly than are the five-membered pyrrolidine ring nitroxides [17] and the oxazolidine nitroxides are intermediate. For this reason, intrinsic rates of reduction of the different spin labels were determined in $CHCl_3$/MeOH (2:1

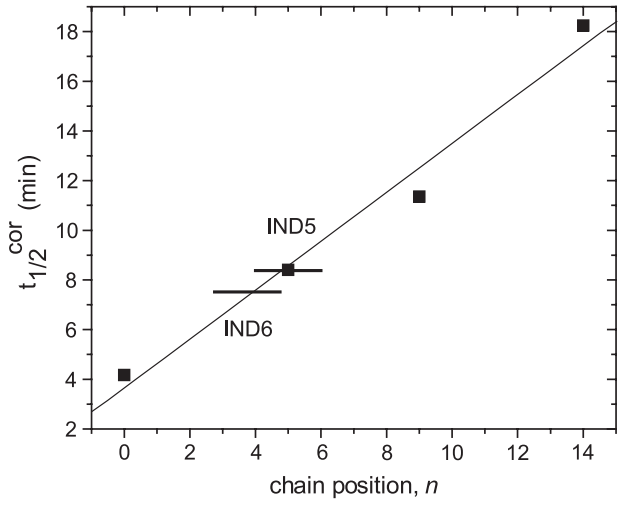

Fig. 8. Diffusional half-times $t_{1/2}^{cor}$ for reduction by 10 mM ascorbate of lipid spin labels, *n*-PCSL and CSL ($n\equiv 0$), in DMPC membranes at 30 °C. Horizontal bars are the corresponding reduction half-times for the INDOL6 and INDOL5 spin-labelled derivatives, as indicated. Half-times are corrected for differences in intrinsic reactivity of the various nitroxides.

v/v) solutions that were treated with 5 mM ascorbate. Measured rates were then extrapolated to 10 mM ascorbate.

The corrected half-times of reduction for INDOL6 and INDOL5 in DMPC membranes are given by the horizontal bars in Fig. 8. Relative to the spin-labelled lipids, the corrected reduction rate of INDOL6 is below that of 5-PCSL, whereas that of INDOL5 is closer to the value for 5-PCSL, i.e., deeper in the membrane. This result is consistent with the conclusions reached from measurements with paramagnetic relaxants, i.e., that the nitroxide groups of INDOL6 and INDOL5 are in the hydrocarbon interior of the membrane, with the indole group anchored at the polar–apolar interface.

4. Conclusions

The 5-(2-indolyl)-2,4-dienoyl V-ATPase inhibitors insert into the bilayer regions of membranes, intercalated between the lipid chains. The nitroxide rings of the spin-labelled derivatives are buried within the hydrophobic interior of the membrane, and the indole moiety is anchored at the polar–apolar interface. The INDOL6 EPR-probe reports sensitively on the fluid lipid environment of the inhibitor, whereas the INDOL5 probe allows direct detection of inhibitor–protein interactions within the membrane.

Acknowledgements

We thank Frau B. Angerstein for synthesis of spin-labelled lipids and Frau B. Freyberg for expert technical assistance. We thank Stephen Ball for communicating his inhibition data. This work was supported under the European Union Framework V, Quality of Life initiative (QLRT-1999-31801).

References

[1] G. Nadler, M. Morvan, I. Delimoge, P. Belfiore, A. Zocchetti, I. James, D. Zembryki, E. Lee-Rycakzewski, C. Parini, E. Consolandi, S. Gagliardi, C. Farina, (2*Z*,4*E*)-5-(5,6-Dichloro-2-indolyl)-2-methoxy-*N*-(1,2,2,6,6-pentamethylpiperidin-4-yl)-2,4-pentadienamide, a novel, potent and selective inhibitor of the osteoclast V-ATPase, Bioorg. Med. Chem. Lett. 8 (1998) 3621–3626.

[2] N. Dixon, T. Páli, S. Ball, M.A. Harrison, D. Marsh, J.B.C. Findlay, T.P. Kee, New biophysical probes for structure–activity analyses of vacuolar-H^+-ATPase enzymes, Org. Biomol. Chem. 1 (2003) 4361–4363.

[3] D. Marsh, A. Watts, Spin-labeling and lipid–protein interactions in membranes, in: P.C. Jost, O.H. Griffith (Eds.), Lipid–Protein Interactions, vol. 2, Wiley-Interscience, New York, 1982, pp. 53–126.

[4] S. Gagliardi, G. Nadler, E. Consolandi, C. Parini, M. Morvan, M.N. Legave, P. Belfiore, A. Zocchetti, G.D. Clarke, I. James, P. Nambi, M. Gowen, C. Farina, 5-(5,6-dichloro-2-indolyl)-2-methoxy-2,4-pentadienamides: novel and selective inhibitors of the vacuolar H^+-ATPase of osteoclasts with bone antiresorptive activity, J. Med. Chem. 41 (1998) 1568–1573.

[5] N. Dixon (2004) Probing inhibition of the vacuolar (H^+) ATPase—targeting osteoporosis, thesis, University of Leeds.

[6] P. Fajer, D. Marsh, Microwave and modulation field inhomogeneities and the effect of cavity Q in saturation transfer ESR spectra. Dependence on sample size, J. Magn. Reson. 49 (1982) 212–224.

[7] D. Marsh, Electron spin resonance: spin labels, in: E. Grell (Ed.), Membrane Spectroscopy. Molecular Biology, Biochemistry and Biophysics, vol. 31, Springer-Verlag, Berlin, 1981, pp. 51–142.

[8] D. Marsh, L.I. Horváth, Structure, dynamics and composition of the lipid–protein interface. Perspectives from spin-labelling, Biochim. Biophys. Acta 1376 (1998) 267–296.

[9] T. Páli, M.E. Finbow, D. Marsh, Membrane assembly of the 16-kDa proteolipid channel from *Nephrops norvegicus* studied by relaxation enhancements in spin-label ESR, Biochemistry 38 (1999) 14311–14319.

[10] D.A. Haas, C. Mailer, B.H. Robinson, Using nitroxide spin labels. How to obtain T_{1e} from continuous wave electron paramagnetic resonance spectra at all rotational rates, Biophys. J. 64 (1993) 594–604.

[11] M.M.E. Snel, D. Marsh, Accessibility of spin-labeled phospholipids in anionic and zwitterionic bilayer membranes to paramagnetic relaxation agents. Continuous wave power saturation EPR studies, Biochim. Biophys. Acta 1150 (1993) 155–161.

[12] M.S. Weiss, U. Abele, J. Weckesser, W. Welte, E. Schiltz, G.E. Schulz, Molecular architecture and electrostatic properties of a bacterial porin, Science 254 (1991) 1627–1630.

[13] W. Hu, T.A. Cross, Tryptophan hydrogen bonding and electric dipole moments: functional roles in the gramicidin channel and implications for membrane proteins, Biochemistry 34 (1995) 14147–14155.

[14] S.H. White, W.C. Wimley, Experimentally determined hydrophobicity scale for proteins at membrane interfaces, Nat. Struct. Biol. 3 (1996) 842–848.

[15] K. Kachel, E. Asuncion-Punzalan, E. London, Anchoring of tryptophan and tyrosine analogs at the hydrocarbon-polar boundary in model membrane vesicles: parallax analysis of fluorescence quenching induced by nitroxide-labeled phospholipids, Biochemistry 34 (1995) 15475–15479.

[16] S. Schreier-Muccillo, D. Marsh, I.C.P. Smith, Monitoring the permeability profile of lipid membranes with spin probes, Arch. Biochem. Biophys. 172 (1976) 1–11.

[17] M. Esmann, K. Hideg, D. Marsh, Analysis of thiol-topography in Na,K-ATPase using labelling with different maleimide nitroxide derivatives, Biochim. Biophys. Acta 1112 (1992) 215–225.